Chinese Journal
of Catalysis

Article

Synergistic effect on Au-Pd bimetallic catalyst during oxidation of benzyl alcohol to sodium benzoate

Zhaoyan Zhang, Ying Wang, Xian Li, Wei-Lin Dai*

Department of Chemistry and Shanghai Key Laboratory of Molecular Catalysis and Innovative Materials, Fudan University, Shanghai 200433, China

A B S T R A C T

A series of AuPd/CeO$_2$ bimetallic catalysts with different Au/Pd molar ratios were investigated and their catalytic performance in the oxidation of benzyl alcohol to sodium benzoate and benzoic acid under solvent-free conditions was studied. The supported catalysts were characterized by X-ray diffraction, UV-Vis diffuse reflectance spectroscopy, transmission electron microscopy, and X-ray photoelectron spectroscopy. The Au-Pd nanoparticles were successfully deposited onto CeO$_2$ as a homogeneous alloy. The activity of the bimetallic catalysts was superior to that of the corresponding monometallic catalysts. This improvement was attributed to the synergistic effect between Au and Pd. The catalyst with an Au/Pd molar ratio of 3/1 showed the best catalytic performance (the yield of benzoic acid reached 92%), and it could be easily recovered and reused for more than seven successive reactions without significant loss of activity.

1. Introduction

Supported bimetallic nanoclusters have generated much interest for decades owing to their unique bifunctional and synergistic properties [1–4]. Compared with monometallic systems, the activity and stability of bimetallic catalysts are drastically improved upon addition of the second metallic element, which can affect both the geometry and electronic properties of the pure metal clusters [5–8]. Supported Au-Pd bimetallic catalysts are used to catalyze a number of reactions with outstanding activity such as oxidative elimination of toluenes [9], nitroarene reduction to imine [10], oxidation of primary carbon-hydrogen [11–13], and oxidation of alcohols [14,15]. Recently, the beneficial effect of Au-Pd alloy exerted on Au and Pd catalysts has attracted much attention [16–18]. For example,

Goodman and co-workers [19] examined the surface structure of model catalysts, such as Pd/Au(111) and Pd/Au(100), via the synthesis of vinyl acetate, and demonstrated that Au on Pd resulted in catalysts with greatly improved activity and selectivity. Keane and co-workers [20] examined a significant increase in activity of AuPd/Al$_2$O$_3$ when compared with Au/Al$_2$O$_3$ towards the hydrogenation of *p*-chloronitrobenzene. Hao's group [21] demonstrated that the addition of Pd to Au/SBA-15 catalysts could decrease the size of the gold nanoparticles, resulting in higher activity towards the selective aerobic oxidation of benzyl alcohol. Additionally, Huang's group [22] has reported the effect of the Au/Pd molar ratio of bimetallic AuPd/MgO on the liquid phase oxidation of benzyl alcohol to benzaldehyde. Regardless, to date, the application of Au-Pd bimetallic catalysts in the oxidation of benzyl alcohol to sodium

benzoate and benzoic acid has rarely been reported.

Cerium oxide (CeO_2) is an effective catalyst employed in various organic reactions such as transamidation of amides [23], selective synthesis of esters from nitriles and alcohols [24], preparation of organic carbamates [25], synthesis of *N*-alkyl amides [26], and reduction of NO_x [27]. Because CeO_2 has acid-base and redox properties that are expected to facilitate and promote catalysis performance [28,29], CeO_2 has been used to support Au [30,31], Cu [32], Ru [33,34], Pt [35], and Pd [36] to catalyze diverse inorganic and organic reactions. Moreover, Au/CeO_2 catalyst has been reported to exhibit better catalytic performance than Au/TiO_2 and Au/Fe_2O_3 towards CO oxidation [30]. Therefore, CeO_2 is considered a promising support candidate to load gold and other noble metals.

Sodium benzoate and benzoic acid are important commodity chemicals with wide use as food additives, preservatives, spices, plasticizers, and mordants. As reported, sodium benzoate and benzoic acid can be prepared upon oxidation of benzyl alcohol in a one-pot solvent-free synthesis method that is environmentally friendly, non-toxic, and energy-efficient [37]. A novel efficient $AuAg/TiO_2$ bimetallic catalyst with a high stability was employed in this reaction. The catalyst that was prepared with an Au/Ag molar ratio of 1/3 produced the best catalytic performance. To further improve the catalytic activity and evaluate the synergistic effect between Au and Pd, herein, we report the preparation of $AuPd/CeO_2$ bimetallic catalysts and investigate their catalytic properties towards the oxidation of benzyl alcohol to sodium benzoate and benzoic acid. A series of $AuPd/CeO_2$ catalysts with different Au/Pd molar ratios were obtained and structurally characterized by UV-Vis diffuse reflectance spectroscopy (DRS), transmission electron microscopy (TEM), and X-ray photoelectron spectroscopy (XPS). It was found that the Au-Pd nanoparticles were mainly present as homogeneous alloys and the catalyst prepared with an Au/Pd ratio of 3/1 displayed optimum catalytic performance.

2. Experimental

2.1. Catalyst preparation

Au-Pd bimetallic catalyst with an Au/Pd molar ratio of 1/1 was loaded on different supports, and the synthesis process was as follows. First, Au/support catalyst was prepared by a deposition-precipitation (DP) method using urea as precipitation agent. Then, 1.0 g of support (TiO_2, MnO_2, SnO_2, ZnO, or CeO_2), 9 mL of aqueous $HAuCl_4$ solution (24.3 mmol/L), and 2.6 g of urea were added to 80 mL of H_2O with continuous stirring. The mixture was stirred for 2 h at 353 K, during which the pH value was gradually increased from 3.0 to 8.0. The as-received precipitate was collected by filtration, washed three times with deionized water, and dried overnight at 373 K, followed by calcination for 4 h at 573 K. Then, the Pd species were loaded on the as-synthesized precursor mentioned above using an impregnation (IM) method. Typically, 1.0 g of the as-synthesized precursor was added to 7.2 mL of aqueous $PdCl_2$ solution (56.3 mmol/L) and mixed with 40 mL of H_2O. The resulting slurry was vigorously stirred at 353 K until complete evapora-

tion of water, and the solid material was dried at 373 K, followed by calcination for 4 h at 673 K. The as-synthesized catalyst is denoted as AuPd/MO, where MO represents the support (i.e., TiO_2, MnO_2, SnO_2, ZnO, or CeO_2). It should be noted that the total metal loading and the Au/Pd molar ratio of all AuPd/MO catalysts were controlled at 8 wt% and 1:1, respectively.

Monometallic Au/CeO_2 catalyst was prepared by DP using urea as precipitation agent. First, 1.0 g of CeO_2 (Aldrich), 18 mL of aqueous $HAuCl_4$ solution (24.3 mmol/L), and 5.2 g of urea were added to 80 mL of H_2O with continuous stirring. The mixture was stirred for 2 h at 353 K, during which the pH value was gradually increased from 3.0 to 8.0. The as-received precipitate was collected by filtration, washed three times with deionized water, and dried overnight at 373 K, and calcined for 4 h at 573 K.

Monometallic Pd/CeO_2 catalyst was prepared by IM. First, 1.0 g of CeO_2 was added to 14.5 mL of aqueous $PdCl_2$ solution (56.3 mmol/L) and mixed with 80 mL of H_2O. The resulting slurry was vigorously stirred at 353 K until complete evaporation of water, and the solid material was dried at 373 K, and then calcined for 4 h at 673 K.

The synthesis process of the bimetallic catalysts with different Au/Pd molar ratios was as follows. First, Au/CeO_2 was prepared by DP (similarly to the monometallic Au/CeO_2). Then, $AuPd/CeO_2$ was prepared by IM (similarly to the monometallic Pd/CeO_2), with Au/CeO_2 as the support. The total metal loading was controlled at 8 wt%. The catalysts prepared at varying Au/Pd molar ratios of 3/1, 2/2, and 1/3 are denoted as $3Au1Pd/CeO_2$, $2Au2Pd/CeO_2$, and $1Au3Pd/CeO_2$, respectively.

2.2. Catalyst characterization

The specific surface area of the samples was determined by nitrogen adsorption at 77 K (Micromeritics TriStar ASAP 3000) using the Brunauer-Emmett-Teller (BET) method. The Au and Pd loadings were determined by the inductively coupled plasma atomic emission spectroscopy (ICP-AES, Thermo E. IRIS). The XRD patterns were recorded on a Bruker D8 advance diffractometer with Cu K_α radiation (λ = 0.154 nm), operating at 40 mA and 40 kV. The XPS spectra were recorded under ultra-high vacuum (<10^{-6} Pa) at a pass energy of 93.90 eV on a Perkin Elmer PHI 5000C ESCA system equipped with a dual X-ray source using Mg K_α (1253.6 eV) anode and a hemispherical energy analyzer. All binding energy was calibrated using contaminant carbon (C $1s$ = 284.6 eV) as a reference. The TEM images were obtained on a JOEL JEM 2010 transmission electron microscope. The UV-Vis DRS spectra were collected using a Shimadzu UV-2450 spectrophotometer operating in the scanning range of 200–800 nm using $BaSO_4$ as background.

2.3. Activity test

All the experiments were carried out in a magnetically stirred glass flask under reflux; a mercury thermometer was used to monitor the reaction temperature that was maintained at 453 K using an oil bath. A predetermined quantity of benzyl alcohol (1.08 g) was introduced into the reactor, and then

$AuPd/CeO_2$ (0.05 g) and NaOH (0.5 g) were added. The temperature-controlled reaction mixture was stirred at 800 rpm for 8 h. Following addition of 12 mL of H_2O, the reaction mixture was centrifuged to remove the catalyst. The filtrate was evaporated and crystallized to obtain sodium benzoate (white solid) with purity of >99%.

The as-obtained filtrate was acidified with aqueous HCl solution until a pH value of 2.0 was attained. The resulting mixture was filtered, and benzoic acid (white solid) was obtained with purity of >99%. Finally, the white solid was dried and weighed. Yield (benzyl acid) = ($n_{benzyl\ acid}/n_{benzyl\ alcohol}$) × 100%. For the recycling test, the spent catalyst was washed with dilute aqueous HCl solution thrice and then calcined at 573 K for 4 h.

3. Results and discussion

3.1. Effect of support on the performance of Au-Pd bimetallic catalysts

The catalytic performance is greatly influenced by the support. The specific surface areas, surface acid-base properties, specific surface functional groups, and metal-support interactions or other structural features would affect the catalytic reaction process. In our study, oxidation of benzyl alcohol to sodium benzoate and benzoic acid was examined in the presence of a series of AuPd/MO catalysts (prepared on various supports, MO) to investigate the influence of the support on the catalyst performance. The results are shown in Fig. 1. The MnO_2- and SnO_2-supported Au-Pd bimetallic catalysts that featured higher amounts of basic sites displayed the lowest catalytic performance. The low catalytic properties could be attributed to the excessive amounts of basic sites and the small specific surface areas [38]. Both the TiO_2- and ZnO-supported Au-Pd bimetallic catalysts exhibited higher catalytic properties when compared with the MnO_2- and SnO_2-supported Au-Pd bimetallic catalysts. $AuAg/TiO_2$ catalysts have been reported as a promising catalyst for the transformation of benzyl alcohol to sodium benzoate [39]. However, the yield of sodium benzoate was only about 78%, and the TiO_2 loaded with the Au-Pd bimetallic catalysts was prone to aggregation in the absence of a
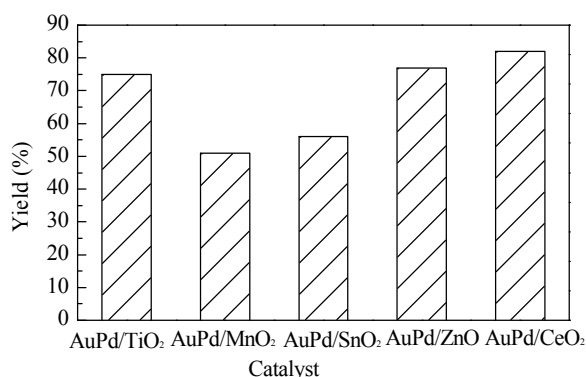
Fig. 1. Catalytic performance of the Au-Pd bimetallic catalysts loaded on different supports, as measured by the benzoic acid yield. Reaction conditions: temperature 453 K, reaction time 8 h, 1.08 g benzyl alcohol, 0.5 g NaOH, and 0.05 g catalyst.

protective agent. The catalytic performance of AuPd/ZnO catalyst is lower when compared with that of $AuPd/CeO_2$, and the poor benzoic acid yield is attributed to the low amounts of acid sites of the ZnO support [40]. In contrast, the CeO_2-supported Au-Pd bimetallic catalysts displayed higher amounts of acid sites and larger specific surface areas. Moreover, it is known that the strong metal-support interaction (SMSI) effect, first reported by Tauster et al. in 1978 [41], greatly enhances the interactions between the Au-Pd bimetallic species and CeO_2 support that subsequently would lead to extended stability of the $AuPd/CeO_2$ catalysts. Thus, the CeO_2 support was chosen in the subsequent studies.

3.2. Catalyst characterization

3.2.1. N_2 adsorption and ICP-AES analyses

The physicochemical properties of the CeO_2-supported Au-Pd bimetallic catalysts with varying Au/Pd molar ratios are listed in Table 1. There were no obvious differences in the pore volume and average pore size, indicating that the introduction of the metal species on the support did not considerably influence the catalyst structure. A slight increase in the BET specific surface areas was observed following loading of the bimetallic species. Based on the ICP-AES analysis, the actual loading of Au or Pd was comparable with the nominal amount, indicative of the successful deposition of Au and Pd on the CeO_2 support.

3.2.2. XRD analysis

The XRD patterns of the monometallic and bimetallic catalysts are shown in Fig. 2. The CeO_2 support is well crystallized showing characteristic diffractogram of fluorite. The *fcc* peaks of Au were observed at $2\theta = 38.2°$, and the intensity of the Au diffraction peak decreased with increasing amounts of Pd. The weak broad peak at $2\theta = 40.1°$, which is characteristic of metallic Pd species, suggests the existence of Pd in the as-prepared Au-Pd bimetallic catalysts (Fig. 2(2)–(5)). A right shift in the Au peaks from $2\theta = 38.2°$ to $2\theta = 38.9°$ was observed, and all the peaks were located between the peaks corresponding to the (111) plane of metallic gold and (111) plane of metallic palladium, suggesting the formation of Au-Pd alloy [42]. Monometallic Pd/CeO_2 (Fig. 2(5)) displayed a diffraction peak corresponding to PdO species formed upon oxidation of Pd during the calcination process. The broad and weak diffraction peak suggests that the size of PdO is very small. Based on the XRD results, both the PdO nanocrystallites and metallic Pd species

Table 1
Physicochemical properties of $AuPd/CeO_2$ catalysts with different Au/Pd molar ratios.

Catalyst	A_{BET} (m²/g)	Content [a] (wt%)		Au particle size [b] (nm)
		Au	Pd	
Au/CeO_2	67.1	7.9	0	4.5
$3Au1Pd/CeO_2$	70.3	5.7	1.5	4.8
$2Au2Pd/CeO_2$	72.6	3.8	3.4	5.4
$1Au3Pd/CeO_2$	71.6	1.9	5.5	5.7
Pd/CeO_2	71.0	0	7.7	5.2

[a] Determined by ICP.
[b] The calculated Au particle size was based on the analysis of more than 200 particles from TEM images.
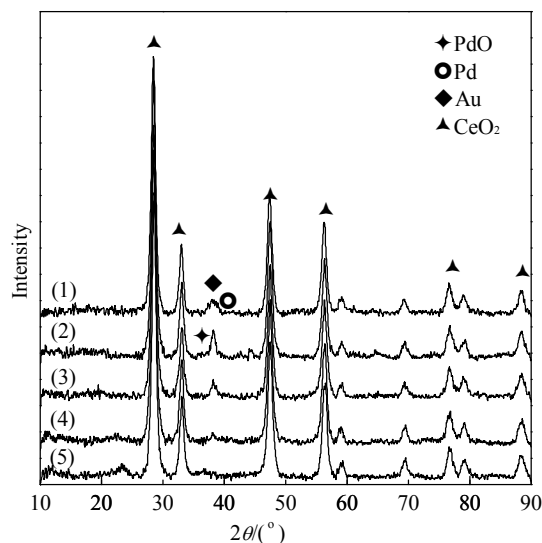
Fig. 2. XRD patterns of AuPd/CeO₂ catalysts with different Au/Pd molar ratios. (1) Au/CeO₂; (2) 3/1; (3) 2/2; (4) 1/3; (5) Pd/CeO₂.

were present in the bimetallic catalysts.

3.2.3. UV-Vis DRS study

Figure 3 shows the UV-Vis DRS spectra of the catalysts with different Au/Pd molar ratios. A weak absorption band at ~570 nm was observed for monometallic Au/CeO₂ catalyst that is due to the surface plasma resonance of the metallic Au particles [43]. As observed, the peak is red-shifted with increasing amounts of Pd, owing to the inter-band transitions of the bimetallic alloy nanoparticles [44–47]. Thus, this finding confirms the formation of an Au-Pd alloy rather than individual and distinct monometallic Au and Pd particles.

3.2.4. TEM results

Figure 4 shows the TEM images and particle size distributions of the AuPd/CeO₂ catalysts with different Au/Pd molar ratios. The metallic particles displayed a narrow size distribu-
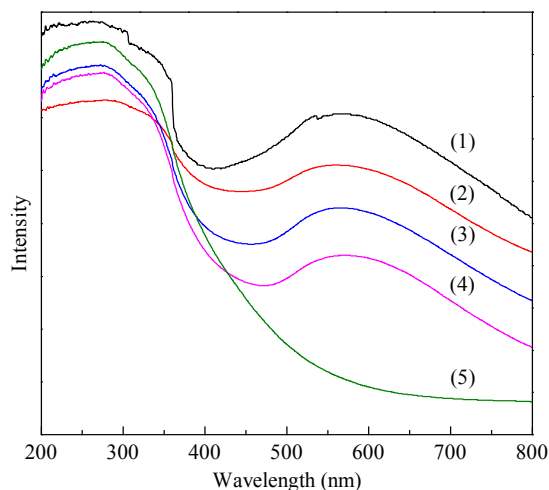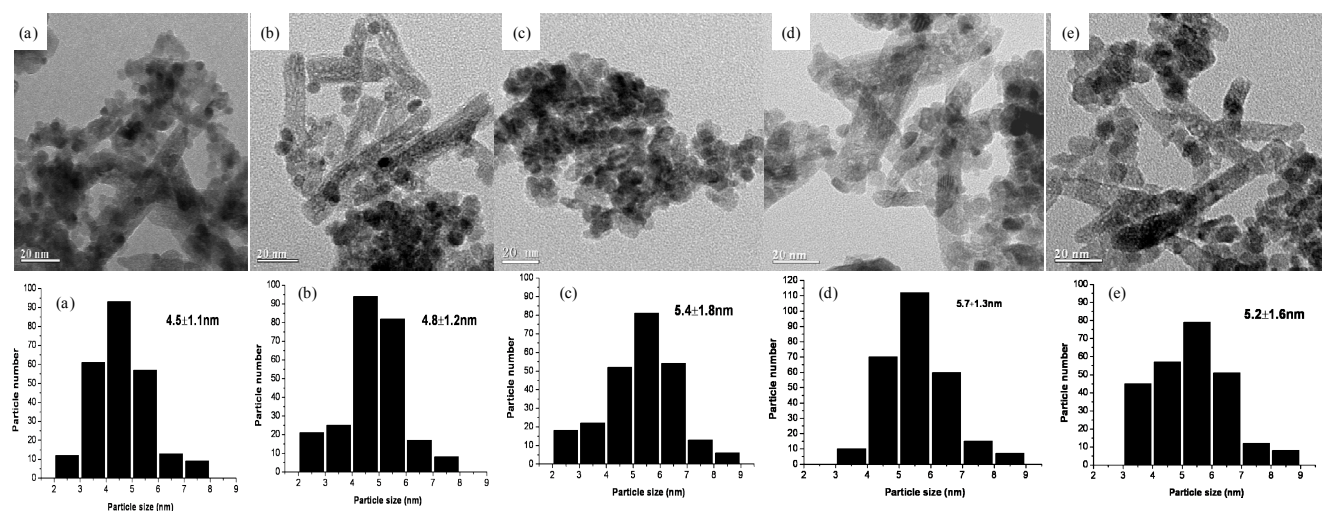

Fig. 3. UV-Vis DRS spectra of AuPd/CeO₂ catalysts with different Au/Pd molar ratios. (1) Au/CeO₂; (2) 3/1; (3) 2/2; (4) 1/3; (5) Pd/CeO₂.

tion and were well dispersed on the surface of the support. The average particle sizes of the monometallic Au/CeO₂ and Pd/CeO₂ catalysts are 4.5 and 5.2 nm, respectively. The morphology of metallic particles was greatly influenced by the addition of the second metal. Compared with the monometallic Au particle, the bimetallic particle size tends to be larger with increasing Pd contents. The mean particle size of the catalysts with Au/Pd ratios of 3/1, 2/2, and 1/3 is 4.8, 5.4, and 5.7 nm, respectively. The 3Au1Pd/CeO₂ catalyst featured the smallest average particle size that is expected to improve the catalytic performance.

3.2.5. XPS analysis

The XPS spectra of the catalysts with different Au/Pd molar ratios are shown in Fig. 5. The corresponding deconvoluted Au 4f and Pd 3d XPS spectra are shown in Figs. 6 and 7. The calculated surface contents of Au and Pd species based on the XPS results are listed in Tables 2 and 3. As observed, the content of

Fig. 4. TEM images and particle size distributions of AuPd/CeO₂ catalysts with different Au/Pd molar ratios. (a) Au/CeO₂; (b) 3/1; (c) 2/2; (d) 1/3; (e) Pd/CeO₂.
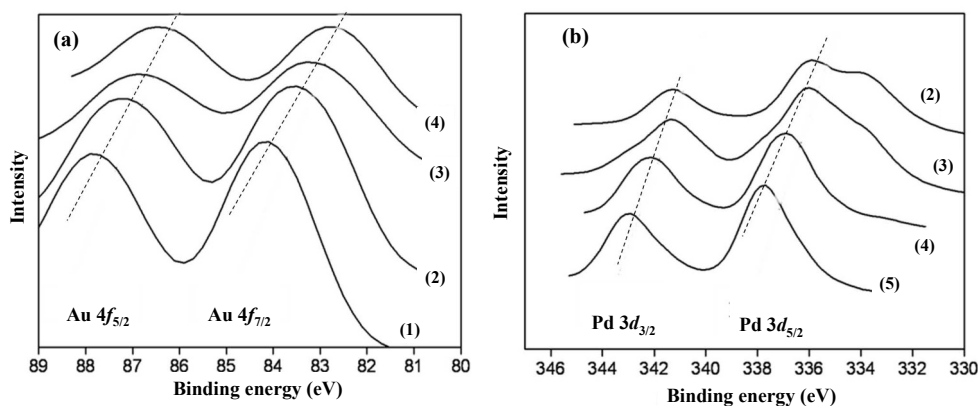
Fig. 5. (a) Au $4f$ and (b) Pd $3d$ XPS spectra of AuPd/CeO$_2$ catalysts with different Au/Pd molar ratios. (1) Au/CeO$_2$; (2) 3/1; (3) 2/2; (4) 1/3; (5) Pd/CeO$_2$.

Au and Pd on the surface of the support is higher than that in bulk (Table 2). However, the surface Au/Pd ratio is slightly higher than the nominal Au/Pd value, implying an enrichment of Au species on the surface of the CeO$_2$ support. The same phenomenon was also reported and discussed in the studies on model bimetallic Pd-Au catalysts [48,49].

Because the peaks corresponding to Au^0 $4d_{5/2}$ (333.8 eV) and Pd^0 $3d_{5/2}$ (334.0 eV), and Au^0 $4f_{5/2}$ (87.7 eV) and Pd^0 $4s$ (88.2 eV) overlap [3,50], the chemical states of the Au and Pd species were examined using the Au $4f_{7/2}$ and Pd $3d_{3/2}$ peaks. Monometallic Au/CeO$_2$ catalyst featured an Au $4f_{7/2}$ peak at 83.7 eV, corresponding to Au$^{\delta+}$ and Au^0 species. Increasing the Pd content resulted in a negative shift of the Au $4f_{7/2}$ peak (Fig. 5(a)) and the surface species of Au changed to Au^0 and Au$^{\delta-}$,

regardless of the studied bimetallic catalyst. Moreover, the amount of Au$^{\delta-}$ increased with increasing Pd amounts (Fig. 5), indicating the transfer of electrons from Pd to Au.

Monometallic Pd/CeO$_2$ catalyst consisted of Pd^0, Pd^{2+}, and Pd^{4+} species on the surface of the support. The appearance of Pd$^{\delta+}$ species is due to the oxidation of partial Pd during the calcination process. When the amount of Au increased, the Pd $3d_{3/2}$ peaks of the bimetallic catalysts shifted to lower binding energy when compared with that in Pd/CeO$_2$ (Fig. 5(b)). The Au $4f_{7/2}$ and Pd $3d_{3/2}$ peak shift to lower binding energy demonstrates the net charge flow between Au and Pd [51–54]. With increasing Au contents, the Pd$^{\delta+}$ species in the bimetallic catalysts were converted into the metallic state (Table 3). Thus, it is believed that Au tends to accept electrons, whereas Pd has
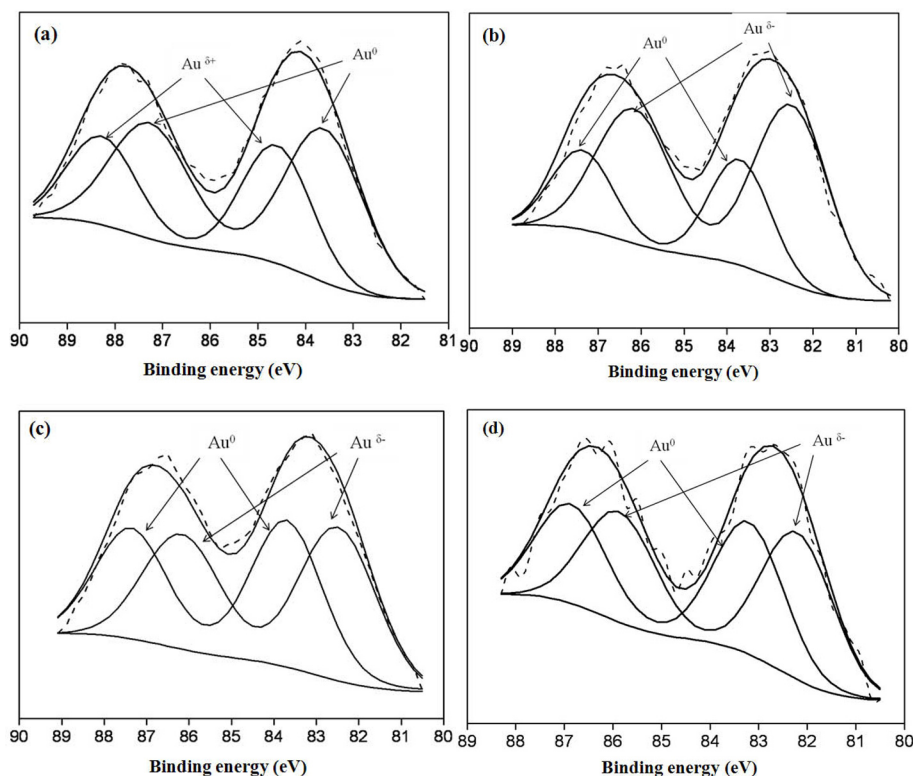

Fig. 6. Au $4f$ XPS spectra of AuPd/CeO$_2$ catalysts with different Au/Pd molar ratios. (a) Au/CeO$_2$; (b) 3/1; (c) 2/2; (d) 1/3.
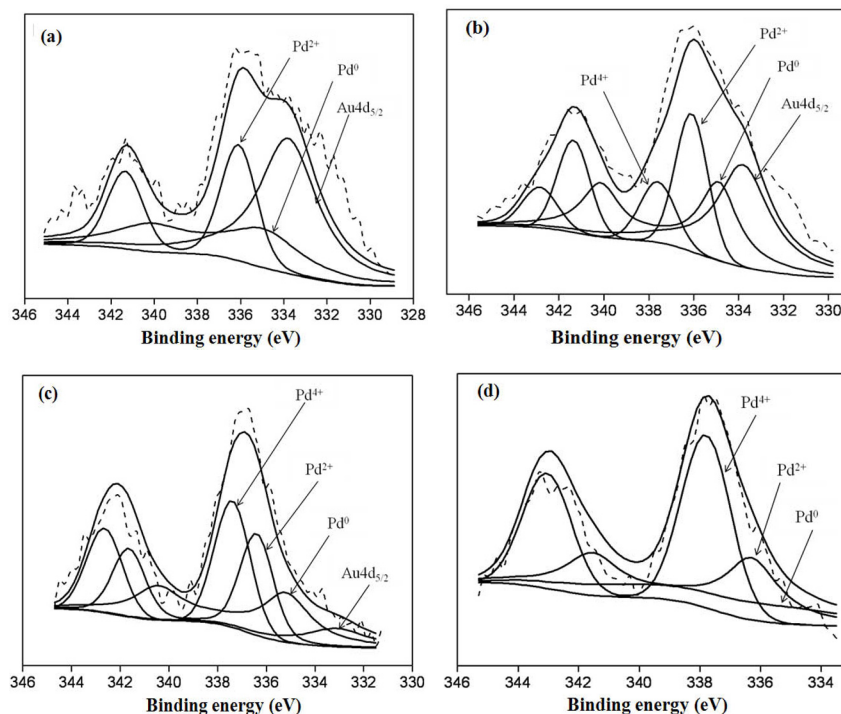
Fig. 7. Pd $3d$ XPS spectra of AuPd/CeO$_2$ catalysts with different Au/Pd molar ratios. (a) 3/1; (b) 2/2; (c) 1/3; (d) Pd/CeO$_2$.

the tendency to lose electrons because of the presence of a synergistic effect between Au and Pd, alluding to the formation of an Au-Pd alloy.

3.3. Catalytic oxidation of benzyl alcohol

The catalytic oxidation of benzyl alcohol to sodium benzoate under solvent-free conditions in the presence of NaOH is known as the Cannizzaro reaction. Benzyl alcohol was oxidized to benzoic aldehyde that instantaneously transformed into sodium benzoate in an alkaline environment.

Table 4 shows the catalytic results using monometallic and bimetallic catalysts towards the oxidation of benzyl alcohol to

sodium benzoate and benzoic acid under solvent-free conditions. Because the desired product was of high purity (selectivity of 100%), the yield was used to evaluate the catalytic activity. As observed, the yields obtained in the presence of the monometallic Au/CeO$_2$ and Pd/CeO$_2$ catalysts are relatively low. Following addition of the second metal, distinctly improved catalytic activity was observed. The catalyst with an Au/Pd ratio of 3/1 displayed the best catalytic performance, with a corresponding yield of 92% achieved after 8 h of reaction. In contrast with Pd/CeO$_2$, the yields generated in the presence of the bimetallic catalysts decreased with increasing Pd amounts. The space time yield (STY) obtained in the presence of the AuPd/CeO$_2$ catalysts was also compared, and the results are shown in Table 4. The STY values markedly increased upon introduction of Pd into the monometallic Au/CeO$_2$ catalyst and reached maxima at an Au/Pd molar ratio of 3/1 (i.e., STY 2.81 h^{-1}), then decreased with further increase in the loading amount of Pd. This indicates the existence of a suitable Au/Pd molar ratio required to generate optimal cata-

Table 2
Surface and bulk compositions of AuPd/CeO$_2$ catalysts obtained from XPS and ICP-AES, respectively.

Catalyst	Surface content (%)		Au/Pd molar ratio	
	Au	Pd	Surface	Bulk
Au/CeO$_2$	9.3	—	—	—
3Au1Pd/CeO$_2$	8.6	2.7	3.2	2.0
2Au2Pd/CeO$_2$	4.0	3.6	1.1	0.6
1Au3Pd/CeO$_2$	3.2	6.4	0.5	0.2
Pd/CeO$_2$	—	8.1	—	—

Table 3
Content of Au and Pd surface species of AuPd/CeO$_2$ catalysts calculated from the XPS results.

Catalyst	Au species (%)			Pd species (%)		
	Au^0	Au$^{\delta-}$	Au$^{\delta+}$	Pd^0	Pd^{2+}	Pd^{4+}
Au/CeO$_2$	61	0	39	0	0	0
3Au1Pd/CeO$_2$	67	33	0	48	52	0
2Au2Pd/CeO$_2$	51	49	0	41	39	20
1Au3Pd/CeO$_2$	42	58	0	30	31	39
Pd/CeO$_2$	0	0	0	19	25	56

Table 4
Reactivity of benzyl alcohol oxidation over AuPd/CeO$_2$ catalysts with different Au/Pd molar ratios.

Catalyst	Conversion (%)	Yield (%)	STY ^{a} (h^{-1})
Au/CeO$_2$	100	70	2.14
3Au1Pd/CeO$_2$	100	92	2.81
2Au2Pd/CeO$_2$	100	83	2.53
1Au3Pd/CeO$_2$	100	72	2.20
Pd/CeO$_2$	100	55	1.68

Reaction conditions: temperature 453 K, reaction time 8 h, 1.08 g benzyl alcohol, 0.5 g NaOH, and 0.05 g catalyst. ^{a} The space time yield (STY) is based on the yield of benzoic acid obtained in the presence of 1 g catalyst per hour; the results were obtained after 8 h of reaction.
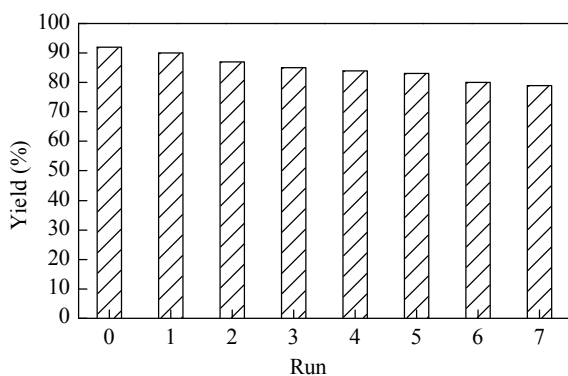
lytic activity.

To examine the stability of the bimetallic catalysts, cycling experiments were conducted using the 3Au1Pd/CeO$_2$ catalyst, and the results are shown in Fig. 8. The bimetallic catalyst was easily recovered and reused for more than seven successive reactions without significant loss in the catalytic activity, indicating the high stability of the as-prepared AuPd/CeO$_2$ catalyst.

Furthermore, the activity of the AuPd/CeO$_2$ catalyst is higher than that of previously studied AuAg/TiO$_2$ (10 h, yield 82%) [37]. Moreover, the use of AuPd/CeO$_2$ catalyst requires lower amounts of catalyst and milder reaction conditions including a lower reaction temperature and a shorter reaction time. Therefore, the as-prepared AuPd/CeO$_2$ is an excellent catalyst candidate for the oxidation of benzyl alcohol to benzoic acid.

3.4.   Synergistic effect of the Au-Pd bimetallic catalysts

Au-based bimetallic nanocatalysts have attracted considerable interest in the past decade owing to their improved sintering resistance and enhanced activity and selectivity. Because Au features a higher electronegativity (2.54) than transition metals, electron transfer from the second metal to Au may occur that will affect the catalytic performance of Au by electronic modification [55]. Wang et al. [56] reported the preparation of graphene-supported Au-Pd bimetallic nanoparticles with excellent catalytic performance towards the selective oxidation of methanol to methyl formate; additionally, their finding pointed out that electron exchange between the Au and Pd species would greatly facilitate the catalytic performance. The considerably lower binding energy of both Au and Pd in Au$_{2.0}$Pd$_{1.0}$/graphene could be attributed to the electron exchange between Au and Pd (i.e., a synergism between the Au and Pd nanoparticles). Wen et al. [57] studied Cu/TiO$_2$-SiO$_2$ catalysts and attributed the blue shift of Cu 2$p_{3/2}$ peak and unchanged Ti 2$p_{3/2}$ peak (which should be blue-shifted as well) binding energy to electron transfer from Ti to Cu. Deng's group [58] also studied the surface electronic characteristics of Ni-B and found that the binding energy of elemental B positively shifted by ~1.1 eV, indicating that B partially donated electrons to Ni. In our study, clear evidence from the XPS measurements was obtained as observed by the decrease in the binding ener-

gy values of the Au 4$f_{7/2}$ levels and increase in the binding energy of the Pd 3$d_{3/2}$ levels in the AuPd/CeO$_2$ catalysts with varying Au/Pd molar ratios (see Table 3). These results strongly suggest the interaction of electrons between the Au and Pd species. Because the physicochemical properties of both the monometallic and bimetallic catalysts are similar, except for the surface electronic properties, with changes in the Au/Pd molar ratio, electron interaction, considered as the synergistic effect of the AuPd/CeO$_2$ catalysts, is believed to play important roles in the high catalytic performance towards the oxidation of benzyl alcohol to benzoic acid [59].

4.   Conclusions

A systematic set of AuPd/CeO$_2$ bimetallic catalysts with different Au/Pd molar ratios have been successfully prepared. The catalysts efficiently catalyzed the oxidation of benzyl alcohol to benzoic acid and sodium benzoate with high yields. Compared with the monometallic catalysts, the catalytic performance of AuPd/CeO$_2$ catalyst was considerably improved upon addition of the second metal. This finding could be ascribed to the formation of homogeneous Au-Pd alloy and the synergistic effect between Au and Pd that influenced the size of the metal particles and their electronic states. Optimal catalytic activity was obtained at an Au/Pd ratio of 3/1. Moreover, this catalyst could be recycled by simple treatment and reused numerous times without significant loss of activity.

References

[1] Moskovits M, Srnova-Sloufova I, Vlckova B. *J Chem Phys,* 2002, 116: 10435

[2] Kim M J, Na H J, Lee K C, Yoo E A, Lee M Y. *J Mater Chem,* 2003, 13: 1789

[3] Xu J, White T, Li P, He C H, Yu J G, Yuan W K, Han Y F. *J Am Chem Soc,* 2010, 132: 10398

[4] Zhang G J, Wang Y E, Wang X, Chen Y, Zhou Y M, Tang Y W, Lu L D, Bao J C, Lu T H. *Appl Catal B,* 2011, 102: 614

[5] Pina C D, Falletta E, Prati L, Rossi M. *Chem Soc Rev,* 2008, 37: 2077

[6] Ishida T, Kinoshita N, Okatsu H, Akita T, Takei T, Haruta M. *Angew Chem Int Ed,* 2008, 47: 9265

[7] Parreira L A, Bogdanchikova N, Pestryakov A, Zepeda T A, Tuzovskaya I, Farias M H, Gusevskaya E V. *Appl Catal A,* 2011, 397: 145

[8] Menegazzo F, Signoretto M, Manzoli M, Boccuzzi F, Cruciani G, Pinna F, Strukul G. *J Catal,* 2009, 268: 122

[9] Cui X J, Shi F, Deng Y Q. *Chem Commun,* 2012, 48: 7586

[10] Xiang Y Z, Meng Q Q, Li X N, Wang J G. *Chem Commun,* 2010, 46: 5918

[11] Wang X G, Venkataramanan N S, Kawanami H, Ikushima Y. *Green Chem,* 2007, 9: 1352

[12] Kesavan L, Tiruvalam R, Ab Rahim M H, bin Saiman M I, Enache D I, Jenkins R L, Dimitratos N, Lopez-Sanchez J A, Taylor S H, Knight D W, Kiely C J, Hutchings G J. *Science,* 2011, 331: 195

[13] Liu H L, Li Y W, Jiang H F, Vargas C, Luque R. *Chem Commun,* 2012, 48: 8431

[14] Enache D I, Edwards J K, Landon P, Solsona-Espriu B, Carley A F, Herzing A A, Watanabe M, Kiely C J, Knight D W, Hutchings G J. *Science,* 2006, 311: 362

Fig. 8. Recyclability of 3Au1Pd/CeO$_2$ towards the catalytic synthesis of sodium benzoate and benzoic acid. Reaction conditions: temperature 453 K, reaction time 8 h, 1.08 g benzyl alcohol, 0.5 g NaOH, and 0.05 g catalyst.

Graphical Abstract

Synergistic effect on Au-Pd bimetallic catalyst during oxidation of benzyl alcohol to sodium benzoate

Zhaoyan Zhang, Ying Wang, Xian Li, Wei-Lin Dai*
Fudan University

A series of AuPd/CeO$_2$ bimetallic catalysts with different Au/Pd molar ratios were successfully prepared and applied in the catalytic oxidation of benzyl alcohol to benzoic acid and sodium benzoate with high yields. The 3Au1Pd/CeO$_2$ catalyst shows optimal performance and was easily recovered and reused for more than seven successive reactions without significant loss of activity, which was attributed to the synergistic effect between Au and Pd.
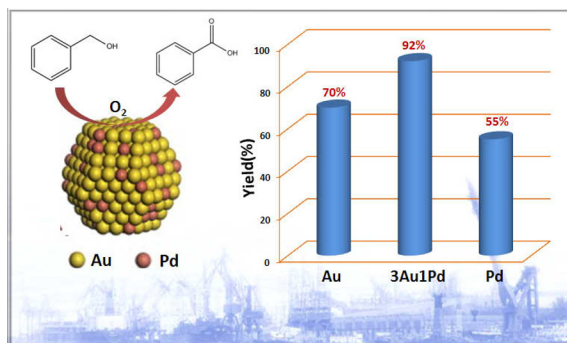
[15] Shi Y, Yang H M, Zhao X G, Cao T, Chen J Z, Zhu W W, Yu Y Y, Hou Z S. *Catal Commun,* 2012, 18: 142

[16] Miedziak P J, Tang Z R, Davies T E, Enache D I, Bartley J K, Carley A F, Herzing A A, Kiely C J, Taylor S H, Hutchings G J. *J Mater Chem,* 2009, 19: 8619

[17] Lee Y W, Kim M, Kim Y, Kang S W, Lee J H, Han S W. *J Phys Chem C,* 2010, 114: 7689

[18] Gu X J, Lu Z H, Jiang H L, Akita T, Xu Q. *J Am Chem Soc,* 2011, 133: 11822

[19] Chen M S, Kumar D, Yi C W, Goodman D W. *Science,* 2005, 310: 291

[20] Cardenas-Lizana F, Gomez-Quero S, Hugon A, Delannoy L, Louis C, Keane M A. *J Catal,* 2009, 262: 235

[21] Ma C Y, Dou B J, Li J J, Cheng J, Hu Q, Hao Z P, Qiao S Z. *Appl Catal B,* 2009, 92: 202

[22] Zhan G W, Hong Y L, Mbah V T, Huang J L, Ibrahim A R, Du M M, Li Q B. *Appl Catal A,* 2012, 439-440: 179

[23] Tamura M, Tonomura T, Shimizu K, Satsuma A. *Green Chem,* 2012, 14: 717

[24] Tamura M, Tonomura T, Shimizu K, Satsuma A. *Green Chem,* 2012, 14: 984

[25] Honda M, Sonehara S, Yasuda H, Nakagawa Y, Tomishige K. *Green Chem,* 2011, 13: 3406

[26] Tamura M, Tonomura T, Shimizu K, Satsuma A. *Appl Catal A,* 2012, 417-418: 6

[27] Krishna K, Seijger G B F, van den Bleek C M, Calis H P A. *Chem Commun,* 2002: 2030

[28] Min B K, Friend C M. *Chem Rev,* 2007, 107: 2709

[29] Schubert M M, Hackenberg S, van Veen A C, Muhler M, Plzak V, Behm R J. *J Catal,* 2001, 197: 113

[30] Carrettin S, Concepcion P, Corma A, Lopez Nieto J M, Puntes V F. *Angew Chem Int Ed,* 2004, 43: 2538

[31] Corma A, Domine M E. *Chem Commun,* 2005: 4042

[32] Tada M, Bal R, Mu X D, Coquet R, Namba S, Iwasawa Y. *Chem Commun,* 2007: 4689

[33] Miura H, Wada K, Hosokawa S, Sai M, Kondo T, Inoue M. *Chem Commun,* 2009: 4112

[34] Sato T, Komanoya T. *Catal Commun,* 2009, 10: 1095

[35] Concepcion P, Corma A, Silvestre-Albero J, Franco V, Chane-Ching J Y. *J Am Chem Soc,* 2004, 126: 5523

[36] Matsumura Y, Shen W J, Ichihashi Y, Okumura M. *Chem Lett,* 1999: 1101

[37] Wang Y, Zheng J M, Fan K N, Dai W L. *Green Chem,* 2011, 13: 1644

[38] Li X, Zheng J M, Yang X L, Dai W L, Fan K N. *Chin J Catal,* 2013, 34: 1013

[39] Cui Y Y, Wang Y, Fan K N, Dai W L. *Appl Surf Sci,* 2013, 279: 391

[40] Nowicka E, Hofmann J P, Parker S F, Sankar M, Lari G M, Kondrat S A, Knight D W, Bethell D, Weckhuysen B M, Hutchings G J. *Phys Chem Chem Phys,* 2013, 15: 12147

[41] Tauster S J, Fung S C, Garten R L. *J Am Chem Soc,* 1978, 100: 170

[42] Jana D, Dandapat A, De G. *J Phys Chem C,* 2009, 113: 9101

[43] Link S, Wang Z L, El-Sayed M A. *J Phys Chem B,* 1999, 103: 3529

[44] Toshima N, Harada M, Yamazaki Y, Asakura K. *J Phys Chem,* 1992, 96: 9927

[45] Creighton J A, Eadon D G. *J Chem Soc, Faraday Trans,* 1991, 87: 3881

[46] Scott R W J, Wilson O M, Oh S K, Kenik E A, Crooks R M. *J Am Chem Soc,* 2004, 126: 15583

[47] Ferrer D, Torres-Castro A, Gao X, Sepulveda-Guzman S, Ortiz-Mendez U, Jose-Yacaman M. *Nano Lett,* 2007, 7: 1701

[48] Berlowitz P J, Peden C H F, Goodman D W. *J Phys Chem,* 1988, 92: 5213

[49] Yi C W, Luo K, Wei T, Goodman D W. *J Phys Chem B,* 2005, 109: 18535

[50] Han Y F, Zhong Z Y, Ramesh K, Chen F X, Chen L W, White T, Tay Q, Yaakub S N, Wang Z. *J Phys Chem C,* 2007, 111: 8410

[51] Chou T S, Periman M L, Watson R E. *Phys Rev B,* 1976, 14: 3248

[52] Nascente P A P, de Castro S G C, Landers R, Kleiman G G. *Phys Rev B,* 1991, 43: 4659

[53] Deki S, Akamatsu K, Hatakenaka Y, Mizuhata M, Kajinami A. *Nanostruct Mater,* 1999, 11: 59

[54] Jose-Yacaman M, Mejia-Rosales S, Perez-Tijerina E, Blom D A, Allard L F. *Microsc Microanal,* 2006, 12: 772

[55] Wang A Q, Liu X Y, Mou C Y, Zhang T. *J Catal,* 2013, 308: 258

[56] Wang R Y, Wu Z W, Chen C M, Qin Z F, Zhu H Q, Wang G F, Wang H, Wu C M, Dong W W, Fan W B, Wang J G. *Chem Commun,* 2013, 49: 8250

[57] Wen C, Yin A Y, Cui Y Y, Yang X L, Dai W L, Fan K N. *Appl Catal A,* 2013, 458: 82

[58] Li H, Li H X, Dai W L, Wang W J, Fang Z G, Deng J F. *Appl Surf Sci,* 1999, 152: 25

[59] Liu J H, Wang A Q, Chi Y S, Lin H P, Mou C Y. *J Phys Chem B,* 2005, 109: 40

Page numbers refer to the contents in the print version, which include both the English and Chinese versions of the paper. The online version only has the English version. The pages with the Chinese version are only available in the print version.